Journal of Health Engineering and Precision Medicine
Volume 1, Issue 1, 31-42, 2025
e_ISSN: xxxx-xxxx p_ISSN: xxxx-xxxx
https://www.journal.foundae.com/index.php/jhep
DOI : https://doi.org/10.58524/jhep.v1i1.48

Optimization of irradiation direction in x-ray therapy for cervical cancer using phits v 3.341 program

Dhawya Najma Nabilla Ramadhin*
Universitas Pertahanan RI,
INDONESIA

Manmeet Kaur
SAGES, farid nagar, bhilai, Chhattisgarh,
INDIA

Article Info

Article history:

Received: Apr 10, 2025
Revised: May 20, 2025
Accepted: Jun 12, 2025

Keywords:

Cervical cancer
Dose distribution
PHITS V 3.341
Radiation optimization
X-ray therapy

Abstract

Cervical cancer is one of the leading causes of cancer-related deaths among women worldwide. The effectiveness of X-ray therapy is significantly influenced by the direction of radiation used in treatment. This research aims to optimize the direction of X-ray radiation therapy for cervical cancer using the PHITS V 3.341 program. The methods employed in this study include numerical simulations to analyze the dose distribution in cervical tissue. The PHITS V 3.341 program is used to calculate the energy distribution and the dose received by the tissue, considering various radiation parameters. The main assumption in this research is tissue homogeneity and the use of standard radiation parameters. The research findings indicate that optimizing the direction of radiation can enhance treatment effectiveness and reduce side effects. These results are compared with existing clinical data and show good conformity. The main conclusion of this study is that using the PHITS V 3.341 program can aid in planning more effective radiation therapy. Further recommendations include additional research for clinical verification.

To cite this article: Ramadhin, D, N, N. (2025). Optimization of irradiation direction in x-ray therapy for cervical cancer using phits v 3.341 program . *Journal of Health Engineering and Precision Medicine, 1*(1), 31-44

INTRODUCTION

Cancer is a major global health burden characterized by the uncontrolled growth and spread of abnormal cells. It remains one of the leading causes of death worldwide, accounting for approximately 10 million deaths annually [1]. Among women, breast, colorectal, lung, cervical, and thyroid cancers are the most prevalent, while in men, lung, prostate, and colorectal cancers dominate. In Indonesia, cervical cancer ranks second after breast cancer as the most common malignancy among women [2].

Cervical cancer, primarily associated with persistent infection by high-risk human papillomavirus (HPV), remains a significant challenge in developing countries due to limited screening and late diagnosis. Radiotherapy, particularly X-ray–based external beam radiotherapy (EBRT), is the mainstay treatment modality for cervical cancer in Indonesia because of its effectiveness and accessibility. This modality delivers ionizing radiation to destroy malignant cells or inhibit their proliferation while sparing adjacent healthy tissues as much as possible [3]. Accurate dosimetric planning is therefore essential to ensure optimal therapeutic outcomes and minimize complications [4].

Imaging techniques such as 18F-fluorodeoxyglucose positron emission tomography/computed tomography (FDG-PET/CT) are widely used to enhance the precision of treatment planning. FDG-PET/CT enables visualization of tumor metabolism and assessment of treatment response by detecting glucose uptake in active cancer cells, offering superior diagnostic sensitivity compared to conventional CT or MRI [5].

Despite the availability of advanced imaging modalities such as FDG-PET/CT for radiotherapy planning, their integration into quantitative dosimetric simulation remains limited. Current clinical systems primarily rely on conventional dose calculation algorithms, which may not

***Corresponding Author:**
Ramadhin, D, N, N. Universitas Pertahanan RI, Indonesia, Email: jhep.med@gmail.com@gmail.com

fully account for complex particle interactions and energy deposition in heterogeneous tissues. Moreover, few studies have utilized Monte Carlo–based simulation tools such as PHITS to validate or optimize X-ray dose distribution and irradiation time in cervical cancer therapy, particularly within the context of Indonesian clinical settings. This gap highlights the need for simulation-based approaches that can complement imaging data to improve the accuracy and effectiveness of radiotherapy planning.

To improve dose accuracy and optimize irradiation parameters, Monte Carlo–based computational simulations have become integral to radiotherapy research. The Particle and Heavy Ion Transport code System (PHITS) is a powerful simulation tool capable of modeling the transport and interaction of photons, electrons, and heavy ions in complex geometries with high precision [6]. PHITS provides detailed analysis of dose distribution and particle behavior in biological tissues, offering advantages in accuracy and efficiency over other transport codes such as MCNP.

This study employs PHITS to simulate X-ray radiotherapy for cervical cancer, focusing on the analysis of dose distribution and irradiation time. The objective is to evaluate the dosimetric performance of X-ray therapy under various irradiation conditions and identify optimal parameters that maximize tumor control while minimizing radiation exposure to surrounding normal tissues. The outcomes of this study are expected to support the development of more precise and effective radiotherapy planning strategies for cervical cancer treatment in Indonesia [7].

MATERIALS & METHODS

This research utilizes simulation software and specific equipment, including laptop with specifications:

1. Processor: Intel(R) Core(TM) i5-4300U CPU @ 1.90GHz, 2.49 GHz, RAM: 8GB, System type 64-bit operating system, x64-based processor.
2. Particle and Heavy Ions Transport Code System (PHITS) simulation program version 3.341, licensed by JAEA.
3. Notepad++ for writing, inputting, and outputting PHITS code.
4. GSView for reading and displaying the output from PHITS code.

A literature review was conducted to identify relevant studies related to cancer treatment, radiotherapy, dose analysis, and the application of the PHITS simulation program. Previous research has shown that Monte Carlo–based methods provide superior accuracy over analytical dose-calculation algorithms in radiotherapy planning. For instance, Sato et al. (2013) [8] detailed the features and validation of PHITS for particle and heavy-ion transport in heterogeneous media, establishing its credibility in dose simulation. Sato et al. (2015) [9] further demonstrated PHITS's applicability in dosimetric studies within medical physics contexts. Other researchers have applied Monte Carlo simulations to optimize beam geometry and dose uniformity in radiotherapy, though few have used PHITS specifically for X-ray radiotherapy of cervical cancer under local clinical conditions in Indonesia. This review thus collates theoretical and empirical data as reference parameters for the present study. Information on PHITS computational framework was obtained from official documentation by the Japan Atomic Energy Agency (JAEA) at https://phits.jaea.go.jp/.

Modeling the geometry of the patient's organs phantom

This modeling utilizes the Particle and Heavy Ions Transport Code System (PHITS) program with the Monte Carlo method. The Monte Carlo method is a computational technique used to solve difficult or impractical numerical problems that cannot be addressed with conventional deterministic methods. It relies on a series of algorithms that use random experiments to obtain results [10]. The geometry of the cervical cancer patient's body is based on the Phantom from the Oak Ridge National Laboratory (ORNL), representing the average adult American woman [11]. Each organ's composition is accessed from materials specified in ICRP Publication 145 [12]. This study will replicate stage IIA cervical cancer in a 32-year-old female patient using FDG-PET scan imaging.

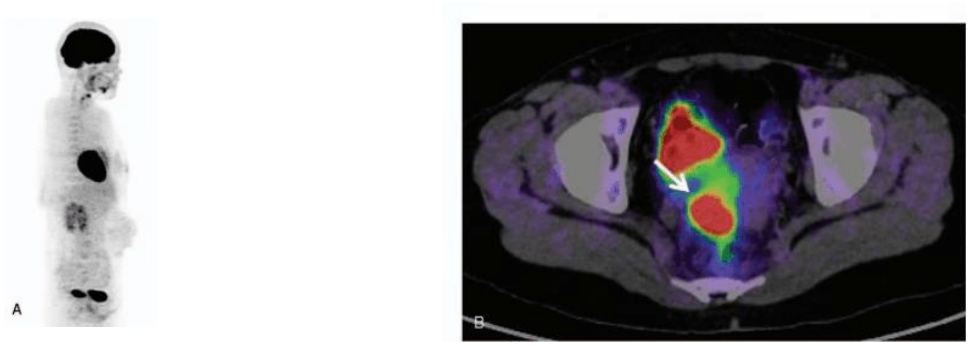

Figure 1. Positron emission tomography (PET) or computed tomography images of a patient with cervical cancer. (A) A typical whole-body 18F-fluorodeoxy-glucose (FDG)-PET image of a patient with cervical cancer. (B) A 32-year-old woman with stage IIA cervical cancer. FDG-PET images clearly show increased focal FDG accumulation (standardized uptake value = 22,43) in the tumor (arrow) [8]. The cancer cell consists of 3 parts called GTV, CTV, dan PTV [11]

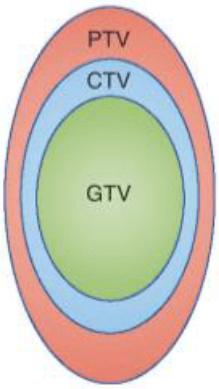

Figure 2. GTV, CTV, PTV position [12]

Each with a size of 1.5, 1.8, and 2.2, with cancer cells (GTV) being spherical with a diameter of 3 cm, CTV being a sheath surrounding GTV with a thickness of 1 cm, and PTV being a sheath surrounding CTV with a thickness of 1 cm. and the combination of GTV, CTV, and PTV is located at a depth of 86.8 cm - 91.2 cm.

Modeling the geometry of the Linear Accelerator (Linac) phantom

The next stage after creating the body geometry is constructing the geometry of the components of the LINAC machine using the PHITS 3.341 program. The LINAC machine modeled is an Elekta brand, type Precise Treatment.

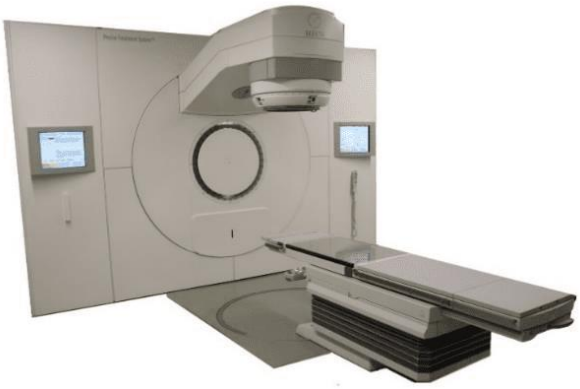

Figure 3. Elekta Precise Linear Accelerator [13]

With its constituent materials as seen in the Table 1.

Table 1. Characteristics of materials used to model the Electa Precise Linac head [14]

Components	Materials	Composition (%)	ρ (g/cm^3)
Target	Tungsten (W)	100	19,3
	Tungsten (W)	95	
Primary collimator	Nikel (Ni)	3,75	18
	Iron (Fe)	1,25	
	Chromium (Cr)	18	
Flattening filter	Nikel (Ni)	74	8,03
	Iron (Fe)	8	
	Tungsten (W)	95	
Secondary collimator	Nickel (Ni)	3,75	18
	Iron (Fe)	1,25	

All the materials above are input in the material section of the PHITS program, forming the geometry of the LINAC machine as shown in Figure 6.

Beam Source

In this study, an electron beam source is used because it utilizes an X-ray machine, specifically a LINAC. As the beam passes through the target (tungsten), it will transform into photon beams that will irradiate the cervical cancer cells until they die. A LINAC with an electron energy of 10 MeV requires a minimum current of 1.8 mA [15]. The following parameters are used in this study.

Table 2. Characteristics of materials used to model the Electa Precise Linac head [14]

No	Parameters	Description
1	Beam Energy	10 MeV
2	Particle	Electron
3	Beam Intensity	0,6653
4	Normalization factor	$1{,}12 \times 10^{16}$
5	Beam size	0,5 cm (radius)
6	Angle irradiation variation	0°, 45°, 90°, 135°, 180°, 225°, 270°, 315°
7	Source distant to the phantom (SSD)	80 cm
8	Number of particles in one run	100.000
9	Number of batches in one rum	50

Dose distribution

The main output generated from programming using PHITS version 3.341 is the dose rate (Gy/s). This dose rate data will be used to calculate the irradiation time and the absorbed dose that the patient will receive. These calculations can then be used to determine the therapy plan for patients diagnosed with stage IIA cervical cancer. According to the Cervical Cancer Management Guidelines issued by the Ministry of Health of the Republic of Indonesia, stage IIA cervical cancer that does not undergo surgery (hysterectomy) and stage IIB can receive external radiotherapy as primary therapy at a dose of 45-50 Gy with 1.8-2 Gy per fraction [16]. If the irradiation time is denoted by t (s), the minimum dose required to kill cancer cells is denoted by $Dmin$ (Gy), and the dose rate is denoted by $Drate$ (Gy/s) [17]. Then Equation 1 can be derived as follows:

$$t(s) = \frac{Dmin\ (Gy)}{Drate\ (Gy/s)} \tag{1}$$

After the irradiation time is determined, the dose received/absorbed by the organ can be calculated. The absorbed dose is calculated using Equation 2 [15].

$$Absorbed\ Dose\ (Gy) = Drate\ (Gy/s) \times t(s) \quad (2)$$

After obtaining the calculated data for the absorbed dose, the next step is to calculate the equivalent dose (H_T) using Equation 3.

$$H_T = \sum_R w_R D_{T,R} \quad (3)$$

When H_T is the equivalent dose, $D_{T,R}$ is the average absorbed dose for the organ or tissue T caused by radiation R. and w_R is the radiation weighting factor for X-rays [18] [19]. The radiation weighting factor for X-rays (photons) is 1 [18] [19]. Finally, the effective dose (E) is calculated using the formula in Equation 4.

$$E = \sum_T w_T \sum_R w_R D_{T,R} = \sum_T w_T H_T \quad (4)$$

Where H_T is the equivalent dose in the organ or tissue T, $D_{T,R}$ is the average absorbed dose for organ or tissue T caused by radiation R, and w_T is the tissue or organ weighting factor [18] [19].

RESULTS AND DISCUSSION

Cervical cancer geometry

The results of the stage IIA cervical cancer replication, based on Figures 1 and 2 and generated using PHITS version 3.341, are presented in Figures 4 and 5.

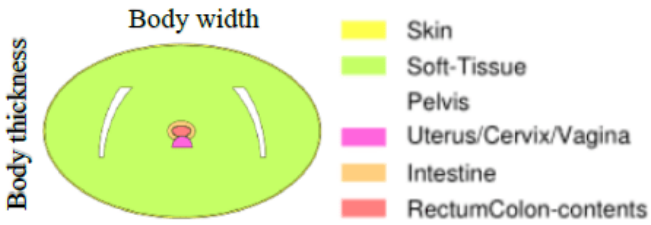

Figure 4. Above side of cervical cancer geometry in 2D

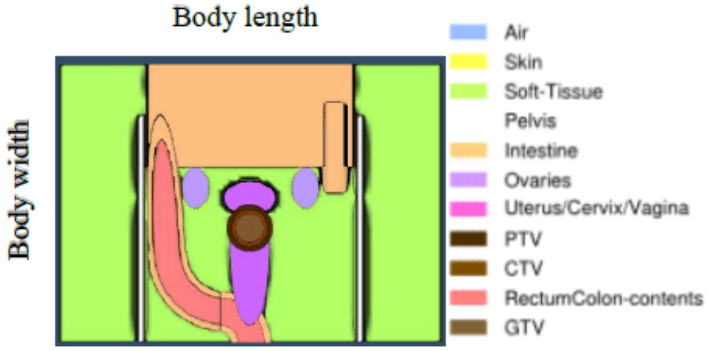

Figure 5. Front side of cervical cancer geometry in 3D

Linear Accelerator geometry

The replication results of the Elekta linear accelerator, including the precise treatment configuration, generated using PHITS version 3.341 and based on Figure 3 and the data in Table 1, are presented in Figure 6.

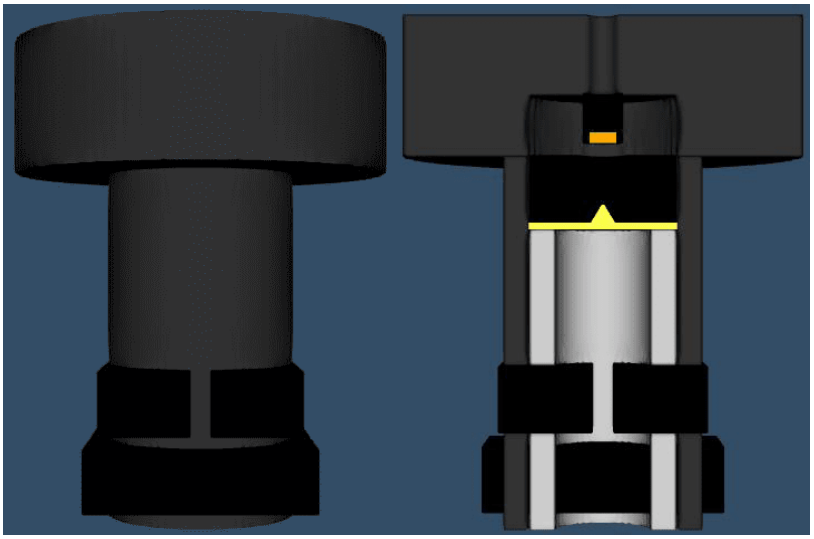

Figure 6. LINAC geometry modelling on 3D

In the figure, black represents the collimator, orange the tungsten target, yellow the flattening filter, gray the gamma shielding, and silver the gamma filter.

Irradiation geometry

Figure 7 illustrates the interaction of the LINAC machine with the electron source, which is directed onto a tungsten target to produce X-rays for cervical cancer treatment, as referenced in Table 2. The X-Y axes represent the beam geometry, with the x-axis spanning −20 to 20 cm (width) and the y-axis 0 to 150 cm (depth). Eight irradiation directions were simulated in this study: Posterior–Anterior (PA, 0°), Right Posterior Oblique (RPO, 45°), Lateral Right (LR, 90°), Right Anterior Oblique (RAO, 135°), Anterior–Posterior (AP, 180°), Left Posterior Oblique (LPO, 225°), Lateral Left (LL, 270°), and Left Anterior Oblique (LAO, 315°).

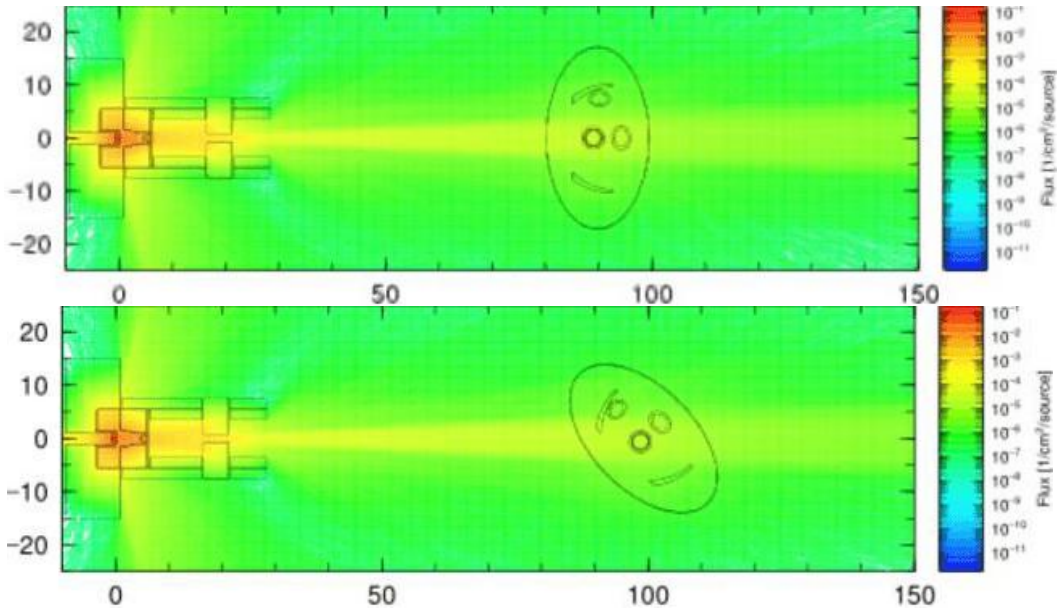

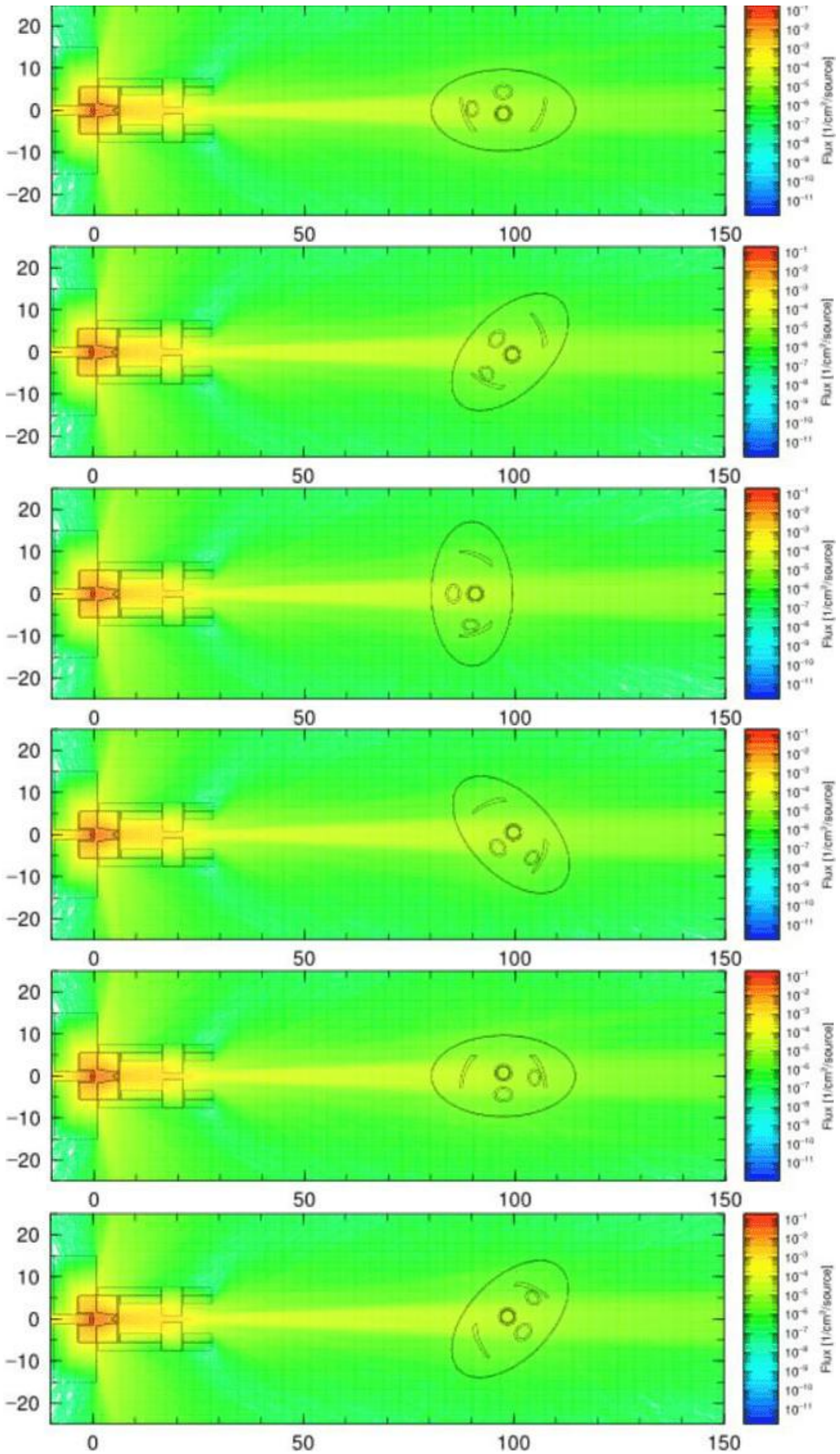

Figure 7. The irradiation geometry in the direction of irradiation 0°,45°,90°,135°,180°,225°,270°,315°

Dose distribution

Figure 8 presents the dose rate distribution along the depth (z-axis) for eight irradiation angles: 0°, 45°, 90°, 135°, 180°, 225°, 270°, and 315°. In all directions, the dose profile exhibits a sharp increase near the surface region (z ≈ 0 cm), corresponding to the point of beam entry, followed by a gradual decrease as the beam penetrates deeper into the tissue. This pattern reflects the characteristic attenuation of X-rays in biological media, where the maximum absorbed dose occurs near the tumor volume, and energy deposition decreases with depth due to scattering and absorption.

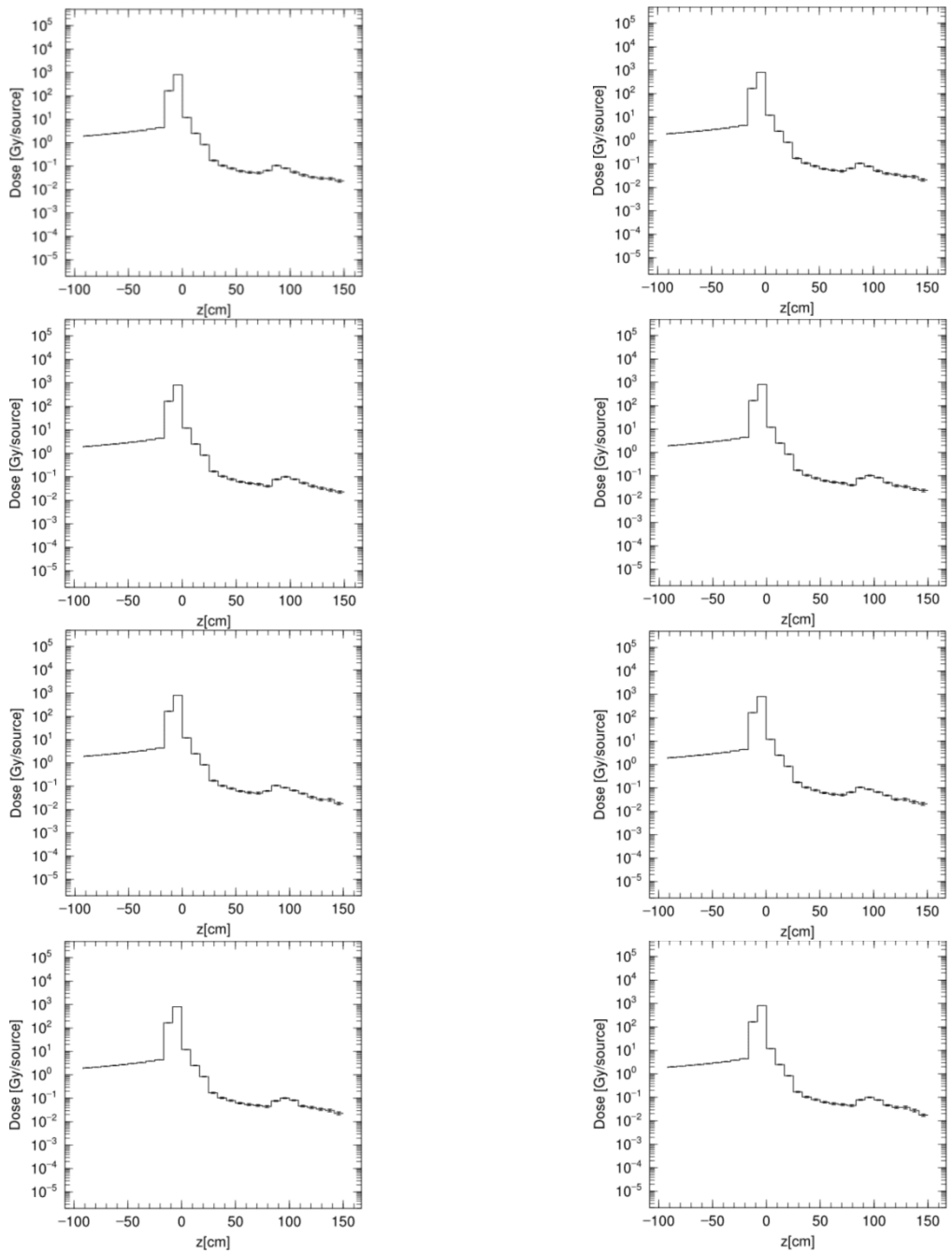

Figure 8. Dose rate graph in the direction of radiation 0°,45°,90°,135°,180°,225°,270°,315°

The similarity of dose distributions across different irradiation angles indicates a uniform beam quality and consistent energy deposition, confirming that the LINAC model accurately reproduces clinical beam characteristics. The superposition of multiple irradiation directions enhances dose uniformity within the target region while reducing excessive exposure to surrounding organs. These findings demonstrate that the simulated treatment geometry effectively mimics

clinical multi-angle external beam radiotherapy for cervical cancer, ensuring optimal tumor coverage and minimal dose to healthy tissue.

Based on formula in Equation 1, 2, 3, and 4, the calculation results for dose rate, irradiation time, absorbed dose, equivalent dose, and effective dose for skin and cancer cell. Besides the skin, the ovaries are also sensitive organs at higher risk from radiation exposure compared to other OARs [23][26]. Therefore, it is necessary to consider the irradiation time, absorbed dose, equivalent dose, and effective dose for the ovaries for analysis as well. All the calculation data can be seen in Table 3.

Table 3. Characteristics of materials used to model the Electa Precise Linac head [14]

	Skin					Cancer cell (CTV, PTV, GTV)					Ovaries				
Angle	**Drate (Gy/s)**	**t (s)**	**Absorbed dose (Gy)**	**H_T (Sv)**	**E (Sv)**	**Drate (Gy/s)**	**t (s)**	**Absorbed dose (Gy)**	**H_T (Sv)**	**E (Sv)**	**Drate (Gy/s)**	**t (s)**	**Absorbed dose (Gy)**	**H_T (Sv)**	**E (Sv)**
0°	0,06	18,8	1,2	1,2	0,5	0,11	18,8	2	2	8,9	0,11	18,8	2	2	8,9
45°	0,04	19,8	0,8	0,8	0,5	0,10	19,8	2	2	13,5	0,10	19,8	2	2	13,5
90°	0,06	22,9	1,4	1,4	0,5	0,09	22,9	2	2	7,5	0,11	22,9	2,5	2,5	9,3
135°	0,04	19,7	0,9	0,9	0,5	0,10	19,7	2	2	12,4	0,10	19,7	2	2	12,4
180°	0,06	18,9	1,2	1,2	0,5	0,11	18,9	2	2	8,8	0,11	18,9	2	2	8,8
225°	0,04	19,4	0,8	0,8	0,5	0,10	19,4	2	2	13,9	0,10	19,4	2	2	13,9
270°	0,07	22,7	1,5	1,5	0,5	0,09	22,7	2	2	7,2	0,11	22,7	2,4	2,4	8,7
360°	0,04	19,9	0,9	0,9	0,5	0,10	19,9	2	2	12,2	0,10	19,9	2	2	12,2

This study aims to determine the most effective irradiation direction based on the shortest irradiation time, high absorbed dose in cancer cells, and low absorbed dose in the skin and ovaries. Based on the data in Table 3, the shortest irradiation time is found in the Posterior-Anterior (PA) / 0° and Anterior-Posterior (AP) / 180° directions, with times of 18.8 seconds and 18.9 seconds, respectively, a difference of 0.1 seconds. The absorbed dose values for the skin, cancer cells, and ovaries are the same at 1.2 Gy, 2 Gy, and 2 Gy, respectively, all within the dose tolerance limits for each organ. The analysis shows that the smallest absorbed dose in the skin occurs in the Right Posterior Oblique (RPO) / 45° and Left Posterior Oblique (LPO) / 225° directions, with a value of 0.8 Gy. The irradiation times for these directions are 19.8 seconds and 19.4 seconds, respectively, a difference of 0.4 seconds. However, the irradiation time for the Posterior-Anterior (PA) / 0° direction is still shorter, at 18.8 seconds. The absorbed dose received by the cancer cells and ovaries in these directions is 2 Gy, within the dose tolerance limits for each organ. Furthermore, the absorbed dose in the ovaries, as seen in Table 3, for six irradiation directions is within the dose tolerance limit for the ovaries, which is 2 Gy per fraction. However, this is not the case for the other two directions: Lateral Right (LR) / 90° and Lateral Left (LL) / 270°. The absorbed doses in the ovaries for these directions are 2.5 Gy and 2.4 Gy, respectively, exceeding the dose tolerance limit for the ovaries.

Precentage Depth Dose

PDD (Precentage Depth Dose) represents the dose distribution at a point on the central axis of the beam within a phantom, usually normalized to Dmax = 100% at the depth of maximum dose (Dmax) [20]. PDD is typically presented in a curve known as a dose profile. The dose profile is one of the curves used to determine the dose distribution received at the target at a specific depth. Accurate dosing is required when targeting to ensure the dose received at the target is maximized according to the pre-treatment plan [21].

Based on the discussion above, there are six effective irradiation directions, excluding the Lateral Right (LR) / 90° and Lateral Left (LL) / 270° directions, where the absorbed dose in the ovaries exceeds the established dose tolerance limits. However, it is still necessary to choose the most optimal irradiation direction based on the criteria mentioned earlier. Among the six effective directions, one has the shortest irradiation time, which is the Posterior-Anterior (PA) / 0° direction, with an irradiation time of 18.8 seconds. Additionally, the absorbed doses for the skin, ovaries, and other OARs are within the dose tolerance limits for each organ [22][23][24][25][26][27][28][29], as shown in Table 4.

Table 4. Characteristics of materials used to model the Electa Precise Linac head [14]

OARs	Dose tolerance limit (Gy)	Absorbed dose (Gy)
Cancer cell	2	2
Uterus/Cervix/Vagina	2	2
Ovaries	2	2
Bladder	3	2
Spine	4	1,22
Pelvis	4	1,22
Rectum	2	2
Colon	3	2
Small intestine	3	2
Healthy tissue	10	1,22
Skin	3	1,22

As shown in Table 4 and Figure 9, the Percentage Depth Dose (PDD) results demonstrate the accuracy of the PHITS 3.341 simulation in replicating clinical dose distributions for stage IIA cervical cancer. Compared with previous studies that used single-beam or simplified geometries, this study provides a more detailed organ-based dose assessment. The absorbed dose in the tumor region (2 Gy) remains within the therapeutic range, while surrounding organs receive lower doses, indicating effective dose confinement and improved protection of healthy tissues.

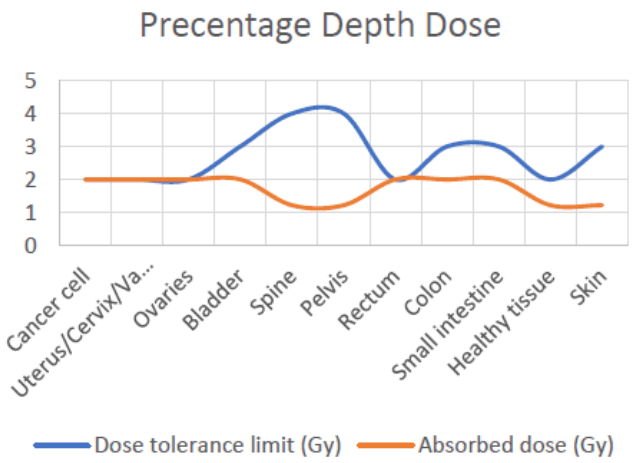

Figure 9. PDD curve

CONCLUSION

This study concludes that the Posterior–Anterior (PA) or 0° irradiation direction provides the most optimal configuration for stage IIA cervical cancer treatment, as it offers the shortest irradiation time, the highest absorbed dose in cancer cells, and the lowest doses in surrounding organs such as the skin and ovaries, all within established dose tolerance limits. The simulation results align with clinical standards, indicating an absorbed dose of 2 Gy per fraction, equivalent to a total of 25 fractions to achieve the therapeutic range of 45–50 Gy required for effective tumor control. The findings also confirm that the irradiation direction significantly affects both the absorbed dose and irradiation time to organs at risk (OARs). Future studies are recommended to incorporate patient-specific anatomical data, evaluate various beam energies and fractionation schemes, and integrate adaptive treatment planning to enhance the accuracy and clinical relevance of PHITS-based radiotherapy simulations.

AUTHOR CONTRIBUTIONS

Dhawya Najma Nabilla Ramadhin was primarily responsible for the conceptualization and design of the study, conducted the PHITS simulations, performed the data analysis and interpretation, and prepared the original draft of the manuscript. Manmeet Kaur contributed to the study design, assisted in data collection and validation from the PHITS simulations, performed critical analysis and visualization of the results, and contributed to the review and editing of the manuscript. Both authors have reviewed and approved the final version of the manuscript and are fully responsible for the content of this work.

REFERENCES

[1] World Health Organization. *Cancer* [Internet]. 2024 [cited 2024 Jun 12]. Available from: https://www.who.int/health-topics/cancer#tab=tab_1

[2] World Health Organization. *Cancer site ranking*. Geneva: WHO; 2022.

[2] Gurram L, Kalra B, Mahantshetty U. Meeting the global need for radiation therapy in cervical cancer - an overview. Semin Radiat Oncol. 2020;30(4):348–54. doi:10.1016/j.semradonc.2020.05.004.

[4] Stavitskii VARV, Yu DONP, AFTAAKA, LLL, AGRR. Dosimetric and mathematical monitoring of the effect of X-ray therapy of cervical cancer. Med Phys. 2009;43.

[5] Skipar K, et al. Risk of recurrence after chemoradiotherapy identified by multimodal MRI and 18F-FDG-PET/CT in locally advanced cervical cancer. Radiother Oncol. 2022;176:17–24. doi:10.1016/j.radonc.2022.09.002..

[6] Sato T, et al. Recent improvements of the Particle and Heavy Ion Transport Code System—PHITS version 3.33. J Nucl Sci Technol. 2024;61(1):127–35. doi:10.1080/00223131.2023.2275736.

[7] Griffin KL, et al. Comparison of out-of-field normal tissue dose estimates for pencil beam scanning proton therapy: MCNP6, PHITS, and TOPAS. Biomed Phys Eng Express. 2022;9:–. doi:10.1088/2057-1976/acaab1.

[8] Sato T, et al. Particle and Heavy Ion Transport code System, PHITS, version 2.52. J Nucl Sci Technol. 2013;50(9):913–23. doi:10.1080/00223131.2013.814553.

[9] Sato T, et al. Overview of Particle and Heavy Ion Transport Code System PHITS. Ann Nucl Energy. 2015;82:110–5. doi:10.1016/j.anucene.2014.08.023.

[10] Takagi H, Sakamoto J, Osaka Y, Shibata T, Fujita S, Sasagawa T. Usefulness of the maximum standardized uptake value for the diagnosis and staging of patients with cervical cancer undergoing PET/CT. Medicine (Baltimore). 2018;97(7):e9856. doi:10.1097/MD.0000000000009856.

[11] Ardana IM, Sardjono Y. Optimization of a neutron beam shaping assembly design for BNCT and its dosimetry simulation based on MCNPX. J Teknol Reaktor Nuklir Tri Dasa Mega. 2017;19(3):121. doi:10.17146/tdm.2017.19.3.3582.

[12] Beaton L, Bandula S, Gaze MN, Sharma RA. How rapid advances in imaging are defining the future of precision radiation oncology. Br J Cancer. 2019;120(8):779–90. doi:10.1038/s41416-019-0412-y.

[13] Puspitasari RA, et al. Analisis kualitas berkas radiasi LINAC untuk efektivitas radioterapi. Jurnal Teknologi Reaktor Nuklir. 2020.

[14] Abou-Taleb WM, Hassan MH, El Mallah EA, Kotb SM. MCNP5 evaluation of photoneutron production from the Alexandria University 15 MV Elekta Precise medical LINAC. Appl Radiat Isot. 2018;135:184–91. doi:10.1016/j.apradiso.2018.01.036.

[15] Zhang ZD, et al. Physical design of a 10 MeV electron LINAC for industrial application and material irradiation effect research. JACoW-IPAC2023. 2022. doi:10.18429/JACoW-IPAC2023-TUPL125.

[16] Andrijono LIOP, et al. Panduan Penatalaksanaan Kanker Serviks. Jakarta: Perhimpunan Onkologi Indonesia; 2014.
[17] Harish AF, Warsono, Sardjono Y. Dose analysis of boron neutron capture therapy (BNCT) treatment for lung cancer based on PHITS. ASEAN J Sci Technol Dev. 2020;35(3):187–94. doi:10.29037/ajstd.545.
[18] Kim CH, Clement CH, eds. *ICRP Publication 145: Annals of the ICRP*. Oxford: ICRP; 2020 [Internet]. Available from: https://www.icrp.org
[19] BATAN. *Proteksi dan Keselamatan Radiasi BATAN*. Jakarta: BATAN; 2014.
[20] Podgorsak EB. External Photon Beams: Physical Aspects. In: Radiation Oncology Physics: A Handbook for Teachers and Students. Vienna: IAEA; 2005.
[21] Mariatul Khiftiyah EH. Analisa kurva percentage depth dose (PDD) dan profile dose untuk lapangan radiasi simetri dan asimetri pada linear accelerator (LINAC) 6 dan 10 MV [Thesis]. Surabaya: Universitas Airlangga; 2014.
[22] BAPETEN. *Peraturan Kepala Badan Pengawas Tenaga Nuklir*. Jakarta: BAPETEN; 2010.
[23] Cefaro GA, Genovesi D, Perez CA, Valentini V. Delineating Organs at Risk in Radiation Therapy. Milan: Springer-Verlag Italia; 2013. doi:10.1007/978-88-470-5257-4.
[24] Bisello S, et al. Dose–volume constraints for organs at risk in radiotherapy (CORSAIR): An all-in-one multicenter multidisciplinary practical summary. Curr Oncol. 2022;29(10):7021–50. doi:10.3390/curroncol29100552.
[25] Jang H, et al. Effective organs-at-risk dose sparing in volumetric modulated arc therapy using a half-beam technique in whole pelvic irradiation. Front Oncol. 2021;11:611469. doi:10.3389/fonc.2021.611469.
[26] Chang DS, Lasley FD, Das IJ, Mendonca MS, Dynlacht JR. Normal tissue radiation responses. In: Basic Radiotherapy Physics and Biology. Cham: Springer; 2014. p. 265–75. doi:10.1007/978-3-319-06841-1_26.
[27] Emami D. Tolerance of normal tissue to therapeutic radiation. Int J Radiat Oncol Biol Phys. 2013.
[28] Gerhard SG, et al. Organ at risk dose constraints in SABR: A systematic review of active clinical trials. Pract Radiat Oncol. 2021;11(4):e355–65. doi:10.1016/j.prro.2021.03.005.
[29] Kementerian Kesehatan Republik Indonesia. *Pedoman Nasional Pelayanan Kedokteran Tata Laksana Kanker Paru* (Keputusan Menteri Kesehatan Republik Indonesia No. HK.01.07/MENKES/1438/2023). Jakarta: Kemenkes RI; 2023.